Published in final edited form as:
Nat Neurosci. 2013 July ; 16(7): 934–941. doi:10.1038/nn.3408.

Synaptic mechanisms of adaptation and sensitization in the retina

Anton Nikolaev, **Kin-Mei Leung**, **Benjamin Odermatt**, and **Leon Lagnado**
Medical Research Council Laboratory of Molecular Biology, Cambridge, UK.

Abstract

Sensory systems continually adjust the way stimuli are processed. What are the circuit mechanisms underlying this plasticity? We investigated how synapses in the retina of zebrafish adjust to changes in the temporal contrast of a visual stimulus by imaging activity *in vivo*. Following an increase in contrast, bipolar cell synapses with strong initial responses depressed, whereas synapses with weak initial responses facilitated. Depression and facilitation predominated in different strata of the inner retina, where bipolar cell output was anticorrelated with the activity of amacrine cell synapses providing inhibitory feedback. Pharmacological block of GABAergic feedback converted facilitating bipolar cell synapses into depressing ones. These results indicate that depression intrinsic to bipolar cell synapses causes adaptation of the ganglion cell response to contrast, whereas depression in amacrine cell synapses causes sensitization. Distinct microcircuits segregating to different layers of the retina can cause simultaneous increases or decreases in the gain of neural responses.

Sensory systems adjust their input-output relation according to the recent history of the stimulus[1]. A common alteration is a decrease in the gain of the response to a constant feature of the input, termed adaptation. Many examples of adaptation occur in the visual system[2,3]. For instance, some retinal ganglion cells (RGCs) produce their strongest responses just after light intensities change in space or time, but the response declines if the visual scene stabilizes[4,5]. The advantage of adaptation is that it prevents saturation of the response to strong stimuli and allows for continued signaling of future increases in stimulus strength[1,6–8]. But adaptation comes at a cost: a reduced sensitivity to a future decrease in stimulus strength. A recent study[8] demonstrated a strategy by which the retina compensates for this loss of information: while some RGCs adapt following a strong stimulus, a second population gradually becomes sensitized. Together, these two opposing forms of plasticity improve the overall rate of information transfer through the population of RGCs when the statistics of the stimulus fluctuates.

What are the circuit mechanisms underlying adaptation and sensitization in the retina? One of the most intensively studied examples has been the decreased sensitivity to temporal contrast after an increase in the variance of light (contrast adaptation), and accumulated evidence indicates that a key mechanism is a decrease in excitatory synaptic transmission from bipolar cells to RGCs[4,7,9–13]. The simultaneous sensitization of a subset of RGCs has only recently been demonstrated and the circuit mechanisms remain to be discovered[8]. We

Correspondence should be addressed to L.L. (II1@mrc-lmb.cam.ac.uk).

AUTHOR CONTRIBUTIONS: A.N., B.O. and L.L. designed the study. A.N., K.-M.L. and B.O. carried out the experiments. A.N., K.-M.L., B.O. and L.L. analyzed measurements. A.N., K.-M.L., B.O. and L.L. wrote the manuscript.

COMPETING FINANCIAL INTERESTS: The authors declare no competing financial interests.

Europe PMC Funders Author Manuscripts

used *in vivo* imaging to monitor the activity of bipolar cell and amacrine cell synapses in the inner retina of zebrafish. These connections are important for processing visual signals[14], and it seems likely that their plasticity will contribute to changes in the input-output relation of the retinal circuit[15].

We found opposing changes in the signals that bipolar cells transmit to RGCs after an increase in the temporal contrast: although some terminals depress and adapt, similar numbers of terminals facilitate and sensitize. Facilitation was associated with a gradual increase in presynaptic calcium, and we found that this was caused by depression of the inhibitory feedback that bipolar cell terminals receive from amacrine cells. Variations in the activity of these inhibitory synapses across different strata of the inner retina led to the partial segregation of depressing and facilitating signals transmitted from bipolar cells. These results illustrate a general mechanism of gain control that may apply to signals transmitted through other neural circuits: a reduction in gain occurs though depression in excitatory synapses, whereas increases in gain reflect depression in inhibitory synapses providing negative feedback.

RESULTS

Depression and facilitation in bipolar cell synapses

To investigate how a change in temporal contrast is signaled to the inner retina, we used two reporters of synaptic activity: sypHy[16] to image synaptic transmission from the population of bipolar cells and SyGCaMP2 (refs. 17,18) to image the presynaptic calcium transient (Fig. 1a). A step of light of constant intensity generated a change in the sypHy signal: ON terminals became brighter in response to the step of light, reflecting the acceleration of vesicle fusion, whereas OFF terminals became dimmer, reflecting a slowing of vesicle release[16,19] (Fig. 1a). After 60 s of adaptation, the intensity was modulated around the same mean with 100% contrast at 5 Hz. There was a large degree of heterogeneity in the responses across the population of bipolar cell terminals (Fig. 1a). For instance, although a large fraction of terminals were excited by the increased variance of the stimulus, some were inhibited (Supplementary Fig. 1 and Supplementary Movie 1).

Although the kinetics of sypHy signals varied between synapses, a clustering algorithm applied to a data set of 5,090 terminals from seven fish revealed clear functional types (Fig. 1b). First, ON and OFF terminals were segregated according to the sypHy signal elicited by steady light. OFF terminals outnumbered ON by 3:1 (ref. 20). Next, we applied the K-means algorithm to separate ON terminals into four groups and OFF terminals into three (Fig. 1c,d), with the number of groups being validated on the basis of the figure of merit (Online Methods and Supplementary Fig. 1a). The dynamics of vesicle release in each group was then quantified as V'_{exo}, the fraction of total vesicles in the terminal released per second (Fig. 1c).

When a step increase in contrast was applied, the strongest initial responses were elicited in ON group 1 and OFF group 1, after which the rate of vesicle release relaxed to a lower steady rate over a few seconds (n = 64 and 341 terminals; Fig. 1c,d). The output from this population of synaptic terminals therefore depressed. The response of terminals in ON group 2 and OFF group 2 was qualitatively different: the increase in contrast caused only a small initial increase in the rate of vesicle release, but, within 1–2 s, the rate began to accelerate and continued to do so over 60 s (n = 95 and 318 terminals; Fig. 1c,d). When applying a 5-Hz stimulus, these facilitating terminals were as prevalent as those that depressed. Group 2 responses represented a specific sensitization to stimulus variance because a return to steady light was signaled by an immediate and large deceleration in the rate of vesicle release.

Finally, group 3 represented a sustained class of terminals that did not respond to rapid modulations in intensity (n = 55 and 143 terminals; Fig. 1c,d).

Synaptic sensitization exhibited persistence (Fig. 1e,f). On returning to low contrast, the rate of vesicle release in group 2 terminals gradually decelerated back to the steady state. A 15-s period of high contrast was sufficient to accelerate vesicle release ~3-fold compared with the steady state (n = 73 terminals from 2 fish; Fig. 1f). Sensitization to temporal contrast has also been observed in the output of the mouse retina, where the mean spike rate of some RGCs can increase ~2-fold after a 15-s exposure to high contrast[8]. Sensitization of bipolar cell synapses therefore occurs under conditions similar to those causing sensitization in RGCs. Opposing forms of plasticity, adaptation and sensitization are therefore already evident in the visual signal as it is transmitted to the inner retina.

A continuum of synaptic changes

Do bipolar cell synapses that depress or facilitate in response to an increase in contrast reflect two distinct subtypes? Or can an individual synapse undergo either form of plasticity, depending on the stimulus? Two observations suggest that the latter was true: the polarity and amplitude of changes in gain were distributed continuously (Fig. 2a) and synapses that depressed at one stimulus frequency could be made to facilitate at another.

We quantified the amplitudes of time-dependent changes in synaptic gain using an adaptation index calculated as the rate of vesicle release immediately after a change in the stimulus divided by the steady-state release rate measured 30 s later. A terminal with an adaptation index greater than 1 is therefore depressing, whereas a terminal with an adaptation index less than 1 is facilitating. The distribution of adaptation indices across all OFF terminals responding to a stimulus of 100% contrast at 5 Hz did not appear to be bimodal (n = 653 terminals from 7 fish; Fig. 2a), indicating that depressing and facilitating synapses reflect two parts of a continuum.

In synapses with an adaptation index greater than 3, an increase in contrast was immediately followed by a strong activation of vesicle release that depressed in ~10–15 s (Fig. 2b). However, in synapses with an adaptation index less than 0.5, the initial response was barely detectable, and facilitation continued throughout the 60-s period of observation. Nonetheless, depression outweighed facilitation 30 s after the increase in contrast such that the average adaptation index across the population of bipolar cell terminals was 1.32 ± 0.05 (n = 244 terminals from 7 fish).

Plasticity in response to changes in temporal correlations

RGCs are capable of responding and adapting not only to changes in the mean or variance of a stimulus, but also to changes in higher order statistics reflecting correlations in space and/or time[21]. To test whether bipolar cells can also sense changes in the temporal pattern of a stimulus, we stepped the frequency of a periodic stimulus from 1 Hz to 5 Hz while keeping the mean and variance constant. Individual bipolar cells display a variety of different transfer functions[20,22,23], so we made this comparison using terminals with a stronger response to 5 Hz than 1 Hz. In terminals of OFF group 1, this transition caused an immediate jump in vesicle release rate followed by depression (n = 66 terminals from 2 fish; Fig. 3a). In other words, bipolar cell synapses in the adapting group rapidly signaled changes in short-term correlations in the stimulus as well as changes in its variance.

The effects of a change in stimulus frequency were qualitatively different in terminals in OFF group 2: these facilitated at 5 Hz, but became depressing at 1 Hz (n = 35 terminals from 2 fish; Fig. 3b and Supplementary Fig. 2). Thus depression or facilitation could occur in the

same terminal, depending on the temporal correlations in the stimulus. This effect was investigated systematically by measuring the relation between adaptation index and the frequency of the stimulus applied from steady light, always at constant contrast (100%). Depression predominated at frequencies below ~5 Hz, whereas there was a progressive shift to facilitation at higher frequencies (n = 911 terminals, 2 fish; Fig. 3c). Furthermore, in individual terminals, there was a strong correlation between the adaptation index measured after a change in contrast and that measured after a change in frequency while contrast was held constant (Fig. 3d).

Together, the results (Figs. 1–3) indicate that the visual signal transmitted from bipolar cells can encode changes in both the variance and temporal pattern of a stimulus, and changes in either of these stimulus features can be followed by adaptation in some terminals and sensitization in others. The plasticity of signal transmission from bipolar cells may have a general role in altering the input-output relation of the retinal circuit.

Adaptation in relation to the presynaptic calcium signal

What are the mechanisms underlying depression and facilitation of transmission from bipolar cells? Short-term alterations in the strength of synaptic connections are often associated with relatively slow changes in calcium concentration in the presynaptic terminal[24]. To investigate whether such changes occurred in bipolar cell synapses, we made *in vivo* measurements of presynaptic calcium using SyGCaMP2 (ref. 18). SypHy and SyGCaMP2 cannot be used simultaneously, as both fluoresce green, so we made separate measurements across all transient OFF terminals responding to contrast; this broad population could be clearly identified according to function using either reporter.

At 1 Hz, most bipolar cell terminals adapted strongly (average adaptation index = 1.9 ± 0.1 with a time constant of 2.9 ± 0.1 s, n = 307 terminals from 4 fish; Fig. 4a). The decrease in release rate reflected a process downstream of calcium influx because the mean amplitude of the presynaptic calcium signal did not change over the period that synaptic depression developed (n = 295 terminals from 5 fish; Fig. 4a). This process is likely to be the activity-dependent depletion of the rapidly releasable pool of vesicles[25–28].

To compare sypHy and SyGCaMP2 signals under conditions in which facilitation predominated, we modulated the stimulus at 5 Hz rather than 1 Hz (n = 659 terminals from 7 fish; Fig. 4b). The presynaptic calcium signal changed distinctively: the initial amplitude was reduced by ~70%, but then gradually increased on a timescale mirroring facilitation (n = 170 terminals from 5 fish). The increase in calcium concentration associated with facilitation began within 1 s of the increase in contrast (Fig. 4b).

We further studied the relation between the degree of facilitation and the presynaptic calcium signal by breaking down the responses of transient OFF terminals according to the layer of the inner plexiform layer (IPL) in which transmission occurred. Release in layers 1 and 2 exhibited a facilitating component to a 5-Hz stimulus (Fig. 4c) and a gradual rise in presynaptic calcium (Fig. 4d). In contrast, OFF terminals in layers 5 and 6 did not display this second phase of sensitization and the average presynaptic calcium signal did not show a secondary rise. These results provide further support for the idea that sensitization of bipolar cell synapses reflects increasing calcium influx.

Facilitation and inhibitory feedback from amacrine cells

The synaptic output of bipolar cells is regulated by feedback from GABAergic amacrine cells[29]. Might sensitization in bipolar cells result from a reduction in these inhibitory signals? To test this disinhibition model, we measured synaptic activity across all classes of

amacrine cells using transgenic zebrafish in which SyGCaMP3 was placed under the control of the *ptf1a* promoter (Fig. 5a)[30]. A step of light or increase in contrast induced distinct responses of opposing polarities in identifiable puncta representing individual synapses or small groups of synapses (Fig. 5a,b). An increase in temporal contrast applied at 5 Hz stimulated amacrine cell synapses strongly, but this response gradually declined over tens of seconds (adaptation index = 1.65 ± 0.20, n = 474 contrast-responding terminals, 5 fish; Fig. 5c). Thus, contrast adaptation in the output of amacrine cells resembled the timescale of facilitation in bipolar cell synapses (n = 370 depressing puncta, 5 fish; Fig. 5d). Furthermore, although a step increase in contrast caused an adapting response in 370 of 474 amacrine cell synapses (78%), only 2% showed facilitation, as represented by an adaptation index substantially less than 1. Thus, sensitization to a stimulus applied at 5 Hz was almost exclusively a property of excitatory transmission in the IPL, whereas inhibitory synapses adapted.

The balance between adaptation and sensitization in the output from bipolar cells varied between different layers of the IPL (Fig. 4), and the disinhibition model predicts that the activity of amacrine cell synapses will also depend on location. When a step increase in contrast was applied, the initial response in layers 1 and 2 was ~3-fold greater than that of synapses in layers 5 and 6 (Fig. 5d). We assessed this behavior more systematically by plotting the ratio of depressing to facilitating bipolar cell terminals in each layer of the IPL against the initial degree of activation of amacrine cell synapses in the same layer (Fig. 5e). The proportion of bipolar cell terminals exhibiting facilitation was correlated with stronger activation of amacrine cell synapses (correlation coefficient = −0.82, $P < 0.05$, n = 6 layers).

The balance between depression and facilitation in bipolar cell terminals was dependent on the frequency of the stimulus (Fig. 3c). If this shift between opposing forms of plasticity is determined by negative feedback from amacrine cells, then these inhibitory signals should also depend on the frequency of the stimulus. This prediction of the disinhibition model was also found to hold. The average SyGCaMP3 signals in amacrine cells responding to a 1-Hz stimulus from layer 2 of the IPL were small and did not change over several tens of seconds (n = 51 terminals, 2 fish; Fig. 5f), but a 5-Hz stimulus generated a larger initial calcium signal, which then depressed (n = 230 terminals, 5 fish).

The spatial and temporal correlations between the synaptic activity of bipolar cells and amacrine cells support the disinhibition model (Fig. 5). To test it further, we used two different experimental manipulations. First, we blocked $GABA_A$ receptors, either by injecting picrotoxin directly into the eye (Fig. 6a) or by bathing the whole fish in 100 μM picrotoxin (Fig. 6b). In both cases, picrotoxin caused a larger initial response to a step increase in contrast and blocked facilitation (average adaptation index increased from 1.05 ± 0.12 to 1.41 ± 0.12, $P < 0.001$, s.d. = 1.17 and 1.38, Wilcoxon rank-sum test, two tailed, n = 95 and 85 OFF terminals, 3 fish). Second, we inhibited the activity of spiking amacrine cells by applying tricaine, a blocker of voltage-gated sodium channels (Fig. 6c). This drug is preferable to tetrodotoxin because it penetrates the larvae very quickly and does not require injection. Tricaine also blocked the facilitating component of the response to a 5-Hz stimulus (adaptation index changed from 1.12 ± 0.09 to 1.76 ± 0.10; $P < 0.001$, s.d. = 0.98 and 0.86, Wilcoxon rank-sum test, two tailed, n = 88 and 64 OFF terminals, 5 fish). We conclude that adaptation and sensitization in the visual signal transmitted from bipolar cells reflects differences in the magnitude and time course of feedback inhibition from amacrine cells. Furthermore, the properties of these inhibitory circuits vary between different layers of the IPL.

Adaptation and sensitization in RGCs

How far are the different forms of plasticity observed in bipolar cells reflected in the activity of ganglion cells? To investigate this question, we generated transgenic fish expressing GCaMP3.5 under the control of the *eno2* promoter (Fig. 7a,b). Calcium signals could be detected in processes through all layers of the IPL in these fish, but the density of labeling did not allow the reliable isolation of signals from individual neurons. We therefore analyzed calcium dynamics on a voxel-by-voxel basis, (Fig. 7c), an approach that was recently used to assess synaptic transmission in the optic tectum[31].

The method of clustering responses in the dendrites of ganglion cells was the same as that applied to synaptic activity in bipolar cells, except that we did not begin by separating ON and OFF signals because zebrafish ganglion cells are predominantly ON-OFF[32]. The functional groups that emerged were analogous to those observed in bipolar cell terminals: group 1 initially responded strongly to the increase in contrast and then adapted, group 2 responded weakly, but then sensitized, and group 3 did not show a clear modulation of calcium after a change in contrast. Adaptation and sensitization of the visual signal transmitted to the IPL was therefore also evident in the dendrites of RGCs.

Partial segregation of depressing and facilitating synapses

Bipolar cells transmit the visual signal through six strata of the IPL[33] (Fig. 8) and this laminar organization has long been thought to reflect the segregation of signals transmitted through a number of parallel-processing channels[34]. This idea has been difficult to explore systematically using electrophysiology, but imaging reporters in synapses and dendrites provide a new approach for investigating the functional anatomy of the IPL.

We examined the distribution of OFF and ON terminals as a function of depth in the IPL (Fig. 8b,e) and of layer (Fig. 8c,f) (n = 824 and 255 terminals, 7 fish). In contrast with findings in other vertebrates, OFF and ON signals were not restricted to sublaminae a and b. For instance, large numbers of OFF terminals were observed in layers 5 and 6, as well as 1 and 2 (Fig. 8c). The coexistence of terminals transmitting ON and OFF signals through much of the IPL may be one mechanism that contributes to the predominance of mixed ON-OFF ganglion cells in zebrafish[32].

The segregation of depressing and facilitating inputs to the IPL was also partial, varying by a factor of ~2–3 for both OFF and ON channels (n varies between 64 and 341 terminals, 7 fish; Fig. 8d,g). As a result, responses averaged across single layers of the IPL contained both depressing and facilitating components (Fig. 4c). The lack of any strict spatial segregation between depressing and facilitating synapses is not surprising given the evidence that responses can shift between these two forms of plasticity depending on the frequency of the stimulus (Fig. 3c). Nonetheless, the preponderance of group 2 synapses in layers 1 and 2 was sufficient to cause the average signal that OFF bipolar cells transmitted to these layers to facilitate after an increase in contrast, whereas the preponderance of group 1 synapses in layer 5 caused depression to dominate (Fig. 4c). Depressing and facilitating responses in dendrites of postsynaptic ganglion cells were also partially segregated, as observed in *eno2-GCaMP3.5* fish (data not shown).

A clearer segregation of signals in the IPL was revealed when we compared the distribution of units classed as transient (groups 1 and 2) and sustained (group 3). These signals overlapped at the input throughout the IPL, as assessed using SyGCaMP2 in bipolar cells (Pearson correlation coefficient = 0.62; n = 34 depth values, 514 transient and 198 sustained terminals, 7 fish; Fig. 8h). But in dendrites of ganglion cells providing the output, transient and sustained signals were strongly segregated, as assessed in *eno2-GCaMP3.5* fish

(Pearson correlation coefficient = −0.51, n = 34 depth values, 191 transient and 131 sustained puncta, 4 fish; Fig. 8i). Sublamina a and b each contained one layer in which RGCs generated sustained responses and one in which the responses were transient. It appears that microcircuits in the IPL act to suppress transmission of transient inputs in some layers and sustained inputs in others.

DISCUSSION

We examined how synapses in the inner retina adjust their responses after an increase in the contrast of the visual stimulus using an *in vivo* preparation that allows activity to be imaged across the whole IPL. This approach revealed an unexpected, but fundamental, feature of the strategy by which the populations of bipolar cells transmit visual information: an increase in temporal contrast or frequency was followed by depression in some synapses and by facilitation in others, and these opposing responses tended to segregate to different layers of the IPL. It has recently been found that, although some RGCs adapt after an increase in stimulus contrast, others gradually sensitize[8]. We found that these opposing forms of plasticity could be traced back to the excitatory signals that RGCs receive from bipolar cells and that they occurred in response to a change in the temporal patterns in a stimulus as well as to a change in variance (Fig. 3).

Mechanisms of synaptic adaptation and sensitization

Much work has focused on the circuit mechanisms of contrast adaptation in the retina[9,10,12,35,36]. Electrophysiological measurements of excitatory synaptic currents in RGCs and amacrine cells indicate that depression of synaptic transmission from bipolar cells is an important mechanism[5,12,13,37], which is consistent with our sypHy measurements of vesicle release (Fig. 1). Depression of bipolar cell synapses might occur by a variety of mechanisms, and these can be considered in two groups: those that lead to inhibition of calcium influx and those that act downstream of the presynaptic calcium signal. The first class of mechanism might include the activation of chloride channels by GABAergic inputs onto these terminals[38], inhibition of voltage-sensitive calcium channels through metabotropic receptors[29,39] or calcium-dependent inactivation[37]. However, we found that synaptic depression was not associated with a decrease in the spatially averaged calcium signal (Fig. 4a,c,d), indicating that it is a result of downstream processes, such as depletion of the pool of rapidly releasable vesicles[26–28,37,40] or a decrease in the calcium sensitivity of the machinery leading to vesicle fusion[26]. Vesicle depletion leading to synaptic depression has been shown to occur in bipolar cells[25–27], and recovery from depletion occurs on a timescale similar to recovery from adaptation[28].

The cellular mechanisms causing the sensitization of RGCs have not been studied, as this phenomenon has only recently been characterized[8]. We found that sensitization of signals transmitted from bipolar cells was correlated with a gradual accumulation of presynaptic calcium (Fig. 4b–d) and three pieces of evidence support the idea that this is a result of decreased GABAergic input from amacrine cells leading to disinhibition. First, amacrine cell synapses were activated most strongly in those layers of the IPL in which signals transmitted through bipolar cells exhibited the largest tendency to facilitate (Fig. 5e). Second, these inhibitory signals depressed on a timescale similar to facilitation in bipolar cells (Fig. 5d). Finally, pharmacological block of inhibitory feedback suppressed facilitation in bipolar cell synapses and enhanced depression (Fig. 6). The gradual rise in presynaptic calcium resulting from disinhibition might also lead to facilitation by accelerating the processes that supply vesicles to the RRP[25,41].

Synaptic plasticity and dynamic encoding in the retina

It is generally thought that the function of contrast adaptation is to counteract response compression, allowing future increases in variance to be encoded in the retinal output[2,7]. What then is the function of facilitation? In thinking about this question, it is important to remember that the visual system must operate in environments of varying contrast and that decreases in contrast, as well as increases, must be sensed. A decrease in contrast sensitivity (adaptation) prevents saturation in an environment of high contrast, but at the cost of less reliable detection of transitions to low contrasts. Conversely, an increase in contrast gain (sensitization) improves the detection of low contrasts, but at the risk of saturating responses to high contrasts. A recent study[8] tested the implications of these ideas by applying signal detection theory to measurements of spike activity across populations of RGCs and found that a mixed population of adapting and sensitizing ganglion cells provides higher overall rates of information transfer than a homogenous population of adapting cells[8]. The central idea to come from our study is that the bipolar cell synapses providing the excitatory drive to RGCs are important for both these forms of plasticity.

The terminals of bipolar cells are key sites of signal integration in the IPL and may be important for regulating the input-output relation of the retinal circuit as it responds to different properties of the visual stimulus. For instance, we found that the signal bipolar cells transmit was sensitive not just to changes in the mean and variance of the visual stimulus, but also to changes in the temporal pattern, and these could also elicit opposing forms of plasticity (Fig. 3). The balance between adaptation and sensitization in different ganglion cells also depended on the responses of amacrine cells in the microcircuits controlling their activity (Figs. 5 and 6). Understanding changes in the performance of the retinal circuit will therefore require a better understanding of plasticity in the different classes of amacrine cell segregating to different layers of the IPL[10]. The observation that amacrine cells underwent depression at high, but not low, frequencies (Fig. 5f) is consistent with a recent study[42] demonstrating that inhibitory inputs to ON bipolar cells in the goldfish retina undergo depression at short interpulse intervals, which is greatly reduced or even turned into facilitation at longer intervals.

Our results illustrate a general mechanism for controlling the amplitude of a signal transmitted through a neural circuit: a reduction in gain occurs though depression in excitatory synapses when these are excited strongly, whereas increases in gain reflect depression in inhibitory synapses, providing negative feedback. It will be interesting to investigate how far this basic scheme applies to other parts of the brain.

ONLINE METHODS

Animals

Tg(–1.8ctbp2:sypHy)lmb fish[16] and *Tg(–1.8ctbp2:SyGCaMP2)lmb* fish[18] were described previously. Tg(*ptf1a:gal4; UAS:SyGCaMP3*) fish were obtained by crossing *Tg(ptf1a:gal4)* (kind gift from M. Parsons, John Hopkins University) to *Tg(UAS:SyGCaMP3)* (kind gift from M. Meyer, King's College London[31]). Fish were maintained on a 14-h:10-h light/dark cycle at 28 °C as described previously[44]. All procedures for animal maintenance and imaging were approved by the Medical Research Council Laboratory of Molecular Biology ethical review committee and the Home Office. Larvae were maintained in fish medium (E2) containing 1-phenyl-2-thiourea at a final concentration of 200 μM (Sigma) from 2 d post-fertilization (dpf) to minimize pigmentation. To further improve optical access to the eye, we used fish homozygous for the *roy orbison* (*roy*) mutation[45]. The basic properties of synaptic adaptation were similar in non-mutant RSY fish.

Imaging

All imaging procedures were described previously[16]. Prior to the experiments, 8–11-dpf larvae were anesthetized by brief exposure to 0.016% tricaine (wt/vol, MS222, Sigma) in E2. Larvae were then immobilized in 2.5% low melting point agarose (Biogene) in E2 on a glass cover slip (0 thickness) and 1 nl of α-bungarotoxin (2 mg ml^{-1}) was injected between the eye and the head to prevent eye movement after recovery from anesthesia during the experiment. Imaging was performed in the afternoon (2–8 p.m.). Images (128 × 128 pixels) were typically acquired every 0.128 s, providing a sampling frequency of 7.8 Hz. The intensity of the excitation laser was low enough to avoid photo-bleaching: the fluorescence decreased by a few percent over a period of several minutes.

Light stimulation

Wide-field light stimuli were delivered using an amber LED (l_{max} = 590 nm, Phillips Luxeon, 350 mA, 3 V) filtered through a 600/10-nm bandpass filter (ThorLabs). Stimuli were delivered through a light guide positioned very close to the fish eye. We did not detect bleed-through of the light stimulus through the GFP filters. In all of the experiments in which the variance of the stimulus was altered, fish were first adapted to the same mean luminance for 1 min. The intensity of the unattenuated light was ~5.5×10^5 photons μm^{-2} s^{-1}. Modulations in light intensity were generated using a custom-built LED driver, which provided linear control by switching the driving current at 10 kHz while adjusting the duty cycle. We chose a 5-Hz stimulation frequency for most of the data shown here because an approximately equal number of bipolar cell terminals exhibited depression and facilitation. We did not use higher frequencies to describe facilitation because the response amplitude of most terminals strongly decreased above 5 Hz.

Image analysis

Images were analyzed using SARFIA, custom-written procedures for IgorPro[43]. Prior to analysis, images were registered to correct movements in the *X* and *Y* directions. Images showing large movements, especially in the *Z* direction, were not analyzed. The analysis was focused on OFF terminals for the following reasons. First, there are more OFF terminals than ON terminals in zebrafish retina[16]. Second, ON cells are more variable. Finally, ON terminals respond to steady light with a very long (several minutes) adaptation.

Cluster analysis

To identify terminals with similar response properties, we used K-means clustering with Pearson correlation as the distance metric. Initially, terminals were divided into ON and OFF groups by their responses to a steady step of light, only using traces with a signal-to-noise ratio (SNR) >2. ON and OFF terminal were then clustered in four and three groups, respectively, using MultiExperiment Viewer software (http://www.tm4.org/mev.html). The number of clusters was decided by using the figure of merit to calculate the minimum number that provided the largest improvement in performance. Prior to applying the K-means algorithm, individual traces were smoothed and normalized so that only the dynamics of the response (rather than the amplitude) determined separation.

Note that the different response types that we describe as groups 1, 2 and 3 represent different parts of a continuum (hence the term group rather than class) and we used the K-means clustering algorithm to objectively recognize these different responses types and then assign all the individual responses to one of these groups. These groups were recognized using a 5-Hz stimulus, but terminals in group 3 (sustained) often responded with modulations in calcium or an increase in mean release rate when the frequency of the

stimulus was reduced to 1 Hz. Contrast-responsive terminals were segregated if the SNR was greater than 2.

Statistical analysis

Statistical analysis was performed using IgorPro. All data are shown as mean ± s.e.m. Differences in adaptation index in the absence or presence of picrotoxin and tricaine were analyzed using two-tailed Wilcoxon rank-sum test. Data before and after drug application were considered to be independent. The non-normal distribution of adaptation index is shown (Fig. 2a) and was validated using a Jarque-Bera test. Equality of variances was tested using Levene's test. Sample sizes were not determined a priori, but are similar to sample sizes in previous studies on ganglion cells approached using multi-electrode array[8,10]. Data collection was not performed blind to the conditions of the experiment, but analysis was performed automatically at all stages using a set of custom-made scripts for IgorPro. This allows avoiding potential human-related bias in the analysis. Data was not randomized. Difference images in Figures 1, 5 and 6 are representative of biological replicates of 3–5 fields of view from five different fish and were masked by multiplying the thresholded version of images shown in Figures 1a, 5a and 7b.

All fish demonstrating robust response to light were included in the analysis. During imaging, we occasionally monitored the heartbeat. If we found that heartbeat was absent or if we observed epileptic-like activity of the neurons, we stopped imaging such larva. No traces were excluded from the analysis. However, we frequently performed analysis on a subset of data (for example, OFF contrast-responding terminals). For the analyses shown in Figure 3d and Wilcoxon rank-sum test, points with adaptation index >5 were excluded from the analysis, as such high values were a result of bad fits required for release rate estimation. Each result was tested from several fields of view obtained from 2–7 fish. We did not find any lack of reproducibility.

Drug application

Pharmacological manipulation was carried out in two different ways. In one set of experiments (Fig. 6a), we injected larva eye with oxygenized Ames' solution containing 100 μM picrotoxin. High-resolution imaging of the retina estimated the ratio between extra- and intracellular space to be 50:1 (F. Esposti and L.L., unpublished observations), yielding a final concentration of 2 μM picrotoxin. Injection of control Ames' solution did not have an effect on depression or facilitation (data not shown). Picrotoxin (Fig. 6b) and tricaine (Fig. 6c) were also added to the bath solution, as they can cross the blood-brain barrier. Injection of picrotoxin into the eye and application to the bath solution produced similar results.

Calculation of vesicle release rates

V'_{exo}, the fraction of total vesicles in the terminal released per second, was calculated from the sypHy signal

$$V'_{\mathrm{exo}}(t) = \frac{1}{19F_{\mathrm{min}}}\left[\frac{dF}{dt} + k_{\mathrm{endo}}(F - F_{\mathrm{min}})\right] \quad (1)$$

where F is the average fluorescence intensity over the terminal at time t, F_{min} is the intensity when the rate of vesicle release is at a minimum and k_{endo} is the rate constant of vesicle retrieval. This relation accounts for the fact that the sypHy signal is affected by both exocytosis and endocytosis of synaptic vesicles. k_{endo} has been measured as 0.1 s^{-1}, both *in vitro*[46–49] and *in vivo*[16]. Estimation of V'_{exo} requires differentiation of the sypHy trace, which in turn amplifies noise, so the responses shown in Figure 1c,d were calculated after

smoothing with the exponential fits shown superimposed[16]. Comparisons of V'_{exo} estimates with and without smoothing are shown in Supplementary Figures 1 and 2.

Equation (1) is a simplified form of the approach used recently to estimate absolute rates of vesicle release from sypHy signals[16]. The calculation of release rate, V_{exo}, starts with the following equation:

$$\frac{dN_{out}}{dt} = V_{exo}(t) - V_{endo}(t) \quad (2)$$

where N_{out} is the number of vesicles fused to the terminal membrane and V_{exo} and V_{endo} are the speeds of exocytosis and endocytosis, respectively. Because

$$V_{endo}(t) = k_{endo} \cdot N_{out}(t) \quad (3)$$

where k_{endo} is the rate constant of endocytosis, the speed of exocytosis is

$$V_{exo}(t) = \frac{dN_{out}}{dt} + k_{endo} \cdot N_{out}(t) \quad (4)$$

Previously[16], we found that

$$N_{out} = \frac{F(t) - N_{total} \cdot F_{vq} - N_{total} \cdot \alpha_{min} \cdot 20 \cdot F_{vq}}{19 \cdot F_{vq}} \quad (5)$$

and

$$F_{vq} = \frac{F_{min}}{N_{total} \cdot (19.\alpha_{min}+1)} \quad (6)$$

where $F(t)$ is fluorescence, N_{total} is the number of vesicles in the terminal, F_{vq} is the fluorescence of a single quenched vesicle, α_{min} is the fraction of sypHy that is unquenched on the surface at rest and F_{min} is the minimum fluorescence when vesicle release is negligible (no light for ON cells and bright light for OFF cells). We have experimentally measured a value of α_{min} = 0.008 (ref. 16) and found that setting α_{min} to zero has negligible effect on estimates of N_{out} and F_{vq}. Thus, N_{out} becomes

$$N_{out} = \frac{F(t) - N_{total} \cdot F_{vq}}{19 \cdot F_{vq}} \quad (7)$$

and

$$F_{vq} = \frac{F_{min}}{N_{total}} \quad (8)$$

After putting equation (8) into equation (7), N_{out} becomes

$$N_{out}(t) = N_{total} \cdot \frac{F(t) - F_{min}}{19 \cdot F_{min}} \quad (9)$$

Defining relative release rate as

$$V'_{\text{exo}}(t) = \frac{V_{\text{exo}}}{N_{\text{total}}} \quad (10)$$

and dividing the left and right parts of equation (4) by N_{out}, we obtain equation (1). Equation (1) shows that an estimate of vesicle release rates requires differentiation of the sypHy signal, which amplifies noise. To limit this difficulty, we fitted the fluorescence responses with a series of single or double exponential functions to obtain non-noisy traces before calculating V'_{exo}. These fits are shown in Figures 1–3. To ensure that the exponential fits did not result in artifactual estimates of contrast or frequency adaptation, we also calculated the adaptation dynamics on the average fluorescence traces without fits (Supplementary Figs. 1 and 2). Our main findings, such as contrast depression and facilitation as well as frequency adaptation, are all evident without this smoothing step and using other reporters of neuronal activity expressed in different cell types.

Generation of *eno2-GCaMP3.5* fish

A 12-kb *eno2* promoter drives protein expression in RGCs, amacrine cells and rod photoreceptors[50]. To express GCaMP3.5 in RGC, we constructed a plasmid DNA to express GCaMP3.5 under the regulation of the *eno2* promoter by replacing the *GFP* gene with the *GCaMP3.5* gene in the pBS-ISce1-eno2-GFP plasmid (a gift from E.A. Burton, University of Pittsburgh) by the domain swapping method. To generate a stable line, we microinjected the *eno2-GCaMP3.5* plasmid flanked by I-Sce1 sites into single cell zebrafish embryos together with I-Sce1. Verification of germline transgenesis was carried out by screening for *eno2-GCaMP3.5*–positive offspring from the microinjected zebrafish. One positive offspring was found and used to establish a stable transgenic line.

Individual RGC growth cones were observed as early as 2 dpf in the chiasm (data not shown). To identify the responses recorded, we characterized the retinal cell types that expressed *eno2-GCaMP3.5* in the transgenic fish using retrograde labeling from the tectum for ganglion cells as well as immunocytochemistry for ganglion and amacrine cells (Supplementary Fig. 3a). For retrograde labeling, Alexa Fluor 594–labeled dextran was loaded to ganglion cells by direct contact with the tracer coated on a fine pin or electrode penetrating into the tectum through the skin dorsally. The labeled larvae were washed and left in E2 medium for up to 2 h to allow sufficient uptake of the tracer into the cell body. Retrograde labeling revealed a 22–28% colocalization with *eno2-GCaMP3.5*–positive cells at 6–7 dpf, indicating that about a quarter of the ganglion cells expressed *eno2-GCaMP3.5* in the retina (Supplementary Fig. 3a). Immunostaining using antibodies to Zn-5 (ZIRC, http://zebrafish.org/zirc/abs/absAll.php?OID=ZDB-ATB-081002-19, 1:500) and parvalbumin (Chemicon, MAB1572, 1:500) to label ganglion and amacrine cells, respectively, revealed that a fraction of Zn-5 positive cells were devoid of *eno2-GCaMP3.5*, whereas parvalbumin-positive amacrine cells colocalized with *eno2-GCaMP3.5* (Supplementary Fig. 3b). These data confirm that *eno2-GCaMP3.5* was also expressed in amacrine cells.

Supplementary Material

Refer to Web version on PubMed Central for supplementary material.

Acknowledgments

We thank all the members of the Lagnado laboratory for discussion. Support for this work was provided by the Medical Research Council and the Wellcome Trust (Programme grant 083220).

References

1. Wark B, Lundstrom BN, Fairhall A. Sensory adaptation. Curr. Opin. Neurobiol. 2007; 17:423–429. [PubMed: 17714934]
2. Kohn A. Visual adaptation: physiology, mechanisms, and functional benefits. J. Neurophysiol. 2007; 97:3155–3164. [PubMed: 17344377]
3. Rieke F, Rudd ME. The challenges natural images pose for visual adaptation. Neuron. 2009; 64:605–616. [PubMed: 20005818]
4. Smirnakis SM, Berry MJ, Warland DK, Bialek W, Meister M. Adaptation of retinal processing to image contrast and spatial scale. Nature. 1997; 386:69–73. [PubMed: 9052781]
5. Wark B, Fairhall A, Rieke F. Timescales of inference in visual adaptation. Neuron. 2009; 61:750–761. [PubMed: 19285471]
6. Laughlin SB. The role of sensory adaptation in the retina. J. Exp. Biol. 1989; 146:39–62. [PubMed: 2689569]
7. Demb JB. Functional circuitry of visual adaptation in the retina. J. Physiol. 2008; 586:4377–4384. [PubMed: 18617564]
8. Kastner DB, Baccus SA. Coordinated dynamic encoding in the retina using opposing forms of plasticity. Nat. Neurosci. 2011; 14:1317–1322. [PubMed: 21909086]
9. Kim KJ, Rieke F. Temporal contrast adaptation in the input and output signals of salamander retinal ganglion cells. J. Neurosci. 2001; 21:287–299. [PubMed: 11150346]
10. Baccus SA, Meister M. Fast and slow contrast adaptation in retinal circuitry. Neuron. 2002; 36:909–919. [PubMed: 12467594]
11. Zaghloul KA, Boahen K, Demb JB. Contrast adaptation in subthreshold and spiking responses of mammalian Y-type retinal ganglion cells. J. Neurosci. 2005; 25:860–868. [PubMed: 15673666]
12. Manookin MB, Demb JB. Presynaptic mechanism for slow contrast adaptation in mammalian retinal ganglion cells. Neuron. 2006; 50:453–464. [PubMed: 16675399]
13. Beaudoin DL, Borghuis BG, Demb JB. Cellular basis for contrast gain control over the receptive field center of mammalian retinal ganglion cells. J. Neurosci. 2007; 27:2636–2645. [PubMed: 17344401]
14. Baccus SA. Timing and computation in inner retinal circuitry. Annu. Rev. Physiol. 2007; 69:271–290. [PubMed: 17059359]
15. Gollisch T, Meister M. Eye smarter than scientists believed: neural computations in circuits of the retina. Neuron. 2010; 65:150–164. [PubMed: 20152123]
16. Odermatt B, Nikolaev A, Lagnado L. Encoding of luminance and contrast by linear and nonlinear synapses in the retina. Neuron. 2012; 73:758–773. [PubMed: 22365549]
17. Dreosti E, Lagnado L. Optical reporters of synaptic activity in neural circuits. Exp. Physiol. 2011; 96:4–12. [PubMed: 20870730]
18. Dreosti E, Odermatt B, Dorostkar MM, Lagnado L. A genetically encoded reporter of synaptic activity in vivo. Nat. Methods. 2009; 6:883–889. [PubMed: 19898484]
19. Lagnado L, Gomis A, Job C. Continuous vesicle cycling in the synaptic terminal of retinal bipolar cells. Neuron. 1996; 17:957–967. [PubMed: 8938127]
20. Ratliff CP, Borghuis BG, Kao YH, Sterling P, Balasubramanian V. Retina is structured to process an excess of darkness in natural scenes. Proc. Natl. Acad. Sci. USA. 2010; 107:17368–17373. [PubMed: 20855627]
21. Hosoya T, Baccus SA, Meister M. Dynamic predictive coding by the retina. Nature. 2005; 436:71–77. [PubMed: 16001064]
22. DeVries SH. Bipolar cells use kainate and AMPA receptors to filter visual information into separate channels. Neuron. 2000; 28:847–856. [PubMed: 11163271]
23. Baden T, Esposti F, Nikolaev A, Lagnado L. Spikes in retinal bipolar cells phase-lock to visual stimuli with millisecond precision. Curr. Biol. 2011; 21:1859–1869. [PubMed: 22055291]
24. Dittman JS, Kreitzer AC, Regehr WG. Interplay between facilitation, depression and residual calcium at three presynaptic terminals. J. Neurosci. 2000; 20:1374–1385. [PubMed: 10662828]

25. Gomis A, Burrone J, Lagnado L. Two actions of calcium regulate the supply of releasable vesicles at the ribbon synapse of retinal bipolar cells. J. Neurosci. 1999; 19:6309–6317. [PubMed: 10414960]
26. Burrone J, Lagnado L. Synaptic depression and the kinetics of exocytosis in retinal bipolar cells. J. Neurosci. 2000; 20:568–578. [PubMed: 10632586]
27. Singer JH, Diamond JS. Vesicle depletion and synaptic depression at a mammalian ribbon synapse. J. Neurophysiol. 2006; 95:3191–3198. [PubMed: 16452253]
28. Ozuysal Y, Baccus SA. Linking the computational structure of variance adaptation to biophysical mechanisms. Neuron. 2012; 73:1002–1015. [PubMed: 22405209]
29. Lukasiewicz PD, Maple BR, Werblin FS. A novel GABA receptor on bipolar cell terminals in the tiger salamander retina. J. Neurosci. 1994; 14:1202–1212. [PubMed: 8120620]
30. Jusuf PR, Harris WA. Ptf1a is expressed transiently in all types of amacrine cells in the embryonic zebrafish retina. Neural Dev. 2009; 4:34. [PubMed: 19732413]
31. Nikolaou N, et al. Parametric functional maps of visual inputs to the tectum. Neuron. 2012; 76:317–324. [PubMed: 23083735]
32. Emran F, et al. OFF ganglion cells cannot drive the optokinetic reflex in zebrafish. Proc. Natl. Acad. Sci. USA. 2007; 104:19126–19131. [PubMed: 18025459]
33. Connaughton VP, Graham D, Nelson R. Identification and morphological classification of horizontal, bipolar, and amacrine cells within the zebrafish retina. J. Comp. Neurol. 2004; 477:371–385. [PubMed: 15329887]
34. Wässle H. Parallel processing in the mammalian retina. Nat. Rev. Neurosci. 2004; 5:747–757. [PubMed: 15378035]
35. Brown SP, Masland RH. Spatial scale and cellular substrate of contrast adaptation by retinal ganglion cells. Nat. Neurosci. 2001; 4:44–51. [PubMed: 11135644]
36. Kim KJ, Rieke F. Slow Na^+ inactivation and variance adaptation in salamander retinal ganglion cells. J. Neurosci. 2003; 23:1506–1516. [PubMed: 12598639]
37. Jarsky T, et al. A synaptic mechanism for retinal adaptation to luminance and contrast. J. Neurosci. 2011; 31:11003–11015. [PubMed: 21795549]
38. Sagdullaev BT, Eggers ED, Purgert R, Lukasiewicz PD. Nonlinear interactions between excitatory and inhibitory retinal synapses control visual output. J. Neurosci. 2011; 31:15102–15112. [PubMed: 22016544]
39. Heidelberger R, Matthews G. Inhibition of calcium influx and calcium current by gamma-aminobutyric acid in single synaptic terminals. Proc. Natl. Acad. Sci. USA. 1991; 88:7135–7139. [PubMed: 1651495]
40. Oesch NW, Diamond JS. Ribbon synapses compute temporal contrast and encode luminance in retinal rod bipolar cells. Nat. Neurosci. 2011; 14:1555–1561. [PubMed: 22019730]
41. Berglund K, Midorikawa M, Tachibana M. Increase in the pool size of releasable synaptic vesicles by the activation of protein kinase C in goldfish retinal bipolar cells. J. Neurosci. 2002; 22:4776–4785. [PubMed: 12077174]
42. Vickers E, Kim MH, Vigh J, von Gersdorff H. Paired-pulse plasticity in the strength and latency of light-evoked lateral inhibition to retinal bipolar cell terminals. J. Neurosci. 2012; 32:11688–11699. [PubMed: 22915111]
43. Dorostkar MM, Dreosti E, Odermatt B, Lagnado L. Computational processing of optical measurements of neuronal and synaptic activity in networks. J. Neurosci. Methods. 2010; 188:141–150. [PubMed: 20152860]
44. Nusslein-Volhard, C.; Dahm, R. Zebrafish. Oxford University Press; Oxford, New York: 2002.
45. Ren JQ, McCarthy WR, Zhang H, Adolph AR, Li L. Behavioral visual responses of wild-type and hypopigmented zebrafish. Vision Res. 2002; 42:293–299. [PubMed: 11809482]
46. Heidelberger R, Zhou ZY, Matthews G. Multiple components of membrane retrieval in synaptic terminals revealed by changes in hydrostatic pressure. J. Neurophysiol. 2002; 88:2509–2517. [PubMed: 12424290]
47. Hull C, von Gersdorff H. Fast endocytosis is inhibited by GABA-mediated chloride influx at a presynaptic terminal. Neuron. 2004; 44:469–482. [PubMed: 15504327]

48. Neves G, Lagnado L. The kinetics of exocytosis and endocytosis in the synaptic terminal of goldfish retinal bipolar cells. J. Physiol. 1999; 515:181–202. [PubMed: 9925888]
49. Neves G, Lagnado L. Visual processing: the devil is in the details. Curr. Biol. 2000; 10:R896–R898. [PubMed: 11137024]
50. Bai Q, Wei X, Burton EA. Expression of a 12-kb promoter element derived from the zebrafish enolase-2 gene in the zebrafish visual system. Neurosci. Lett. 2009; 449:252–257. [PubMed: 19007858]

Europe PMC Funders Author Manuscripts

Europe PMC Funders Author Manuscripts

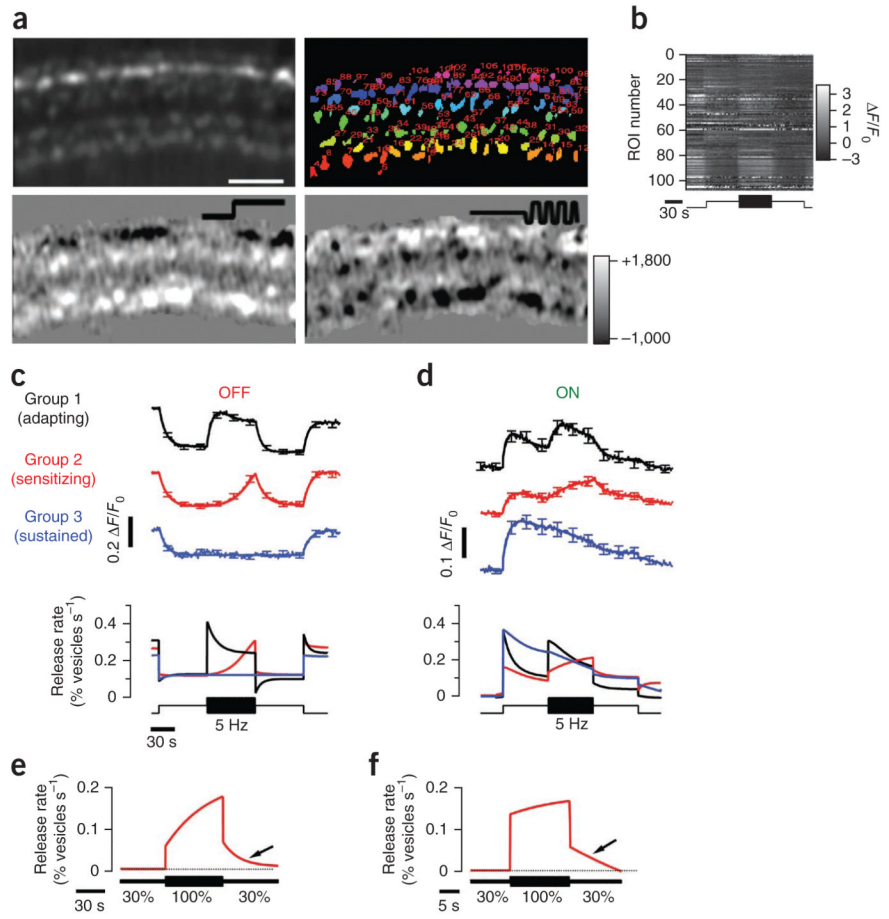

Figure 1. Depressing and facilitating synaptic responses to temporal contrast.

(**a**) Top, field of view showing sypHy in synaptic terminals of bipolar cells and regions of interest (ROIs) marked with different colors. Scale bar represents 15 μm. Bottom, difference images highlighting the change in sypHy fluorescence in response to a step of light and modulation of light intensity at 5 Hz (square wave). Color scale to the right indicates changes in fluorescence for both difference images (arbitrary units). (**b**) Raster plot showing the relative change in fluorescence for each ROI shown in the top right image in **a.** (**c,d**) Different classes of sypHy responses to steady light and contrast in OFF (**c**) and ON (**d**) terminals, distinguished using the K-means clustering algorithm (5,060 terminals from 7 fish). The upper traces show the average sypHy signal in each group, together with the smoothing fits, and the lower graph shows the conversion of these into the relative rate of vesicle release (see Online Methods). The stimulus is shown at the bottom. (**e**) Dynamics of the averaged response of facilitating terminals to contrast increment and decrement (n = 282 terminals, 3 fish) obtained by clustering of all contrast-responding terminals into two classes using a K-means algorithm (only facilitating group is shown). (**f**) Example of responses to contrast increase and decrease as in **e**. The period of high contrast was reduced to 15 s (n = 73 terminals, 2 fish). The mean intensity of the stimulus was 5.5 × 105 photons μm^{-2} s^{-1} at 590 nm. All error bars represent s.e.m.

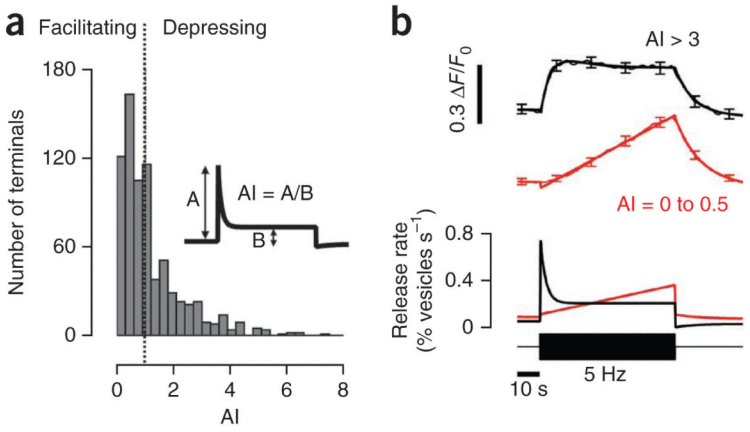

Figure 2. Variations in contrast adaptation across bipolar cell synapses.

(**a**) Distribution of the adaptation index (AI) for the OFF terminals in groups 1 and 2 (*n* = 653 terminals, 7 fish). The inset explains how adaptation index was measured. An adaptation index of less than 1 represents facilitation and an index greater than 1 represents depression (dotted line). Note the broad and monophasic distribution of adaptation index. (**b**) Average response of terminals with adaptation indices of 3–10 (depressing, black trace) and 0–0.5 (facilitating, red trace). The average sypHy responses with smoothing fits are shown above and the conversion to relative release rate is shown below. At the bar, a stimulus of 100% contrast at 5 Hz was applied. All error bars represent s.e.m.

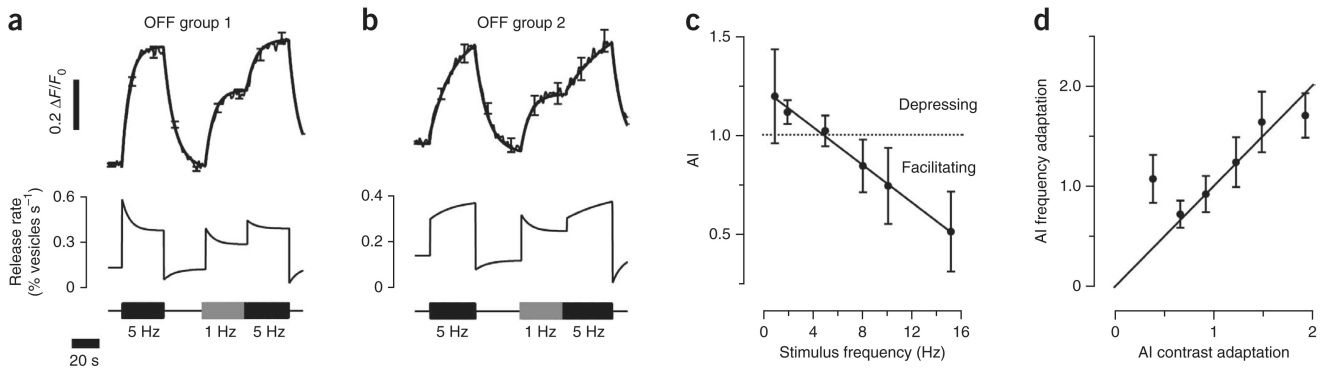

Figure 3. Frequency-dependent plasticity of synaptic transmission from bipolar cells.

(**a**) Terminals in OFF group 1 responding to a change in frequency. The stimulus consisted of a period at 5 Hz, followed by a return to steady light, then a period at 1 Hz, and immediately stepping to 5 Hz. The average sypHy response with smoothing fits is shown above and conversion to release rate is shown below (adaptation index > 1.5, *n* = 66 terminals, 2 fish). (**b**) Terminals in OFF group 2 responding to a change in frequency (adaptation index < 1, *n* = 35 terminals, 2 fish; see Supplementary Fig. 2). (**c**) Average adaptation index as a function of stimulus frequency in OFF terminals responsive to contrast (*n* = 911 terminals, 2 fish). Adaptation index was measured when the stimulus was applied from steady light, always at 100% contrast. Thus, this was not 'frequency adaptation', as both the variance and frequency of the stimulus changed. (**d**) Relation between adaptation index measured in individual terminals after an increase in contrast and after a change in frequency at constant contrast (*n* = 132 terminals, 2 fish). Contrast adaptation was measured at 5 Hz (the first stimulus shown in **a** or **b**). Frequency adaptation was measured from the second stimulus at 5 Hz, delivered immediately after a period of stimulation at 1 Hz. Each point is the binned response from 23 terminals. The line shows equality. All error bars represent s.e.m.

Europe PMC Funders Author Manuscripts

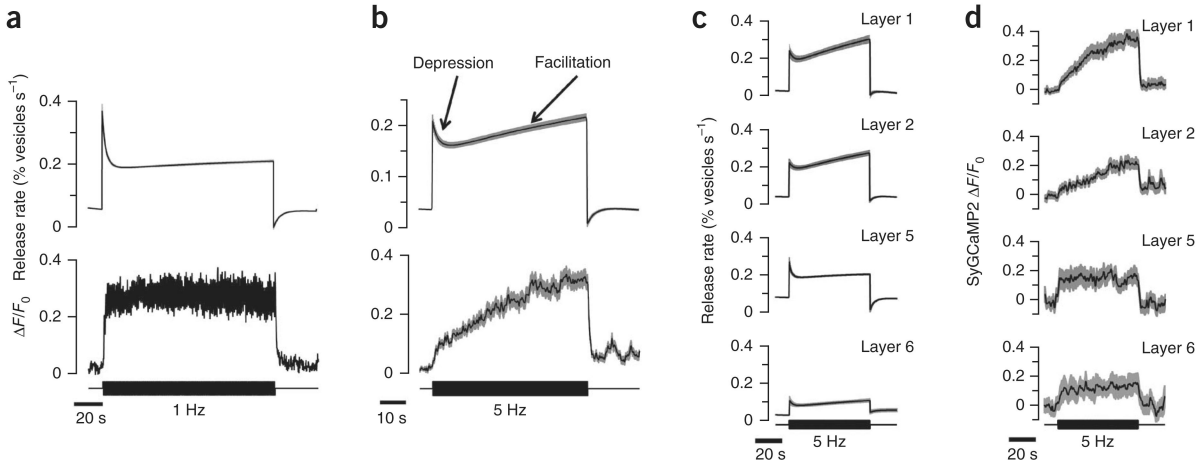

Figure 4. Presynaptic calcium signals associated with depression and facilitation.

(**a**) Average relative release rate (upper trace, *n* = 309 terminals, 4 fish) and SyGCaMP2 signal (middle, *n* = 295 terminals, 5 fish) in two separate series of measurements in OFF terminals responsive to contrast. The stimulus frequency of 1 Hz was chosen to cause a dominance of depression. Note that the SyGCaMP2 signal is steady on the timescale over which synapses depress. (**b**) Stimulation at 5 Hz, chosen to cause an approximately 1:1 ratio between depressing and facilitating synapses (Fig. 1). Average relative release rate (*n* = 659 terminals, 7 fish) and SyGCaMP2 signal (*n* = 170 terminals, 5 fish) in OFF terminals responsive to contrast. Note the gradual increase in presynaptic calcium on the timescale that vesicle release facilitates. (**c**) The average relative release rates of OFF terminals in layers 1, 2, 5 and 6 responding to a 5-Hz stimulus. Terminals insensitive to contrast (group 3) were not included. Facilitating OFF terminals were found predominantly in layers 1 and 2. (**d**) The average SyGCaMP2 signal in OFF terminals in layers 1, 2, 5 and 6 responding to a 5-Hz stimulus. Note that, in layer 5 and 6, the presynaptic calcium levels were steady and depression was the predominant response, whereas there was a gradual rise in presynaptic calcium and a larger proportion of terminals generating a facilitating response in layers 1 and 2. Gray shaded areas indicate s.e.m.

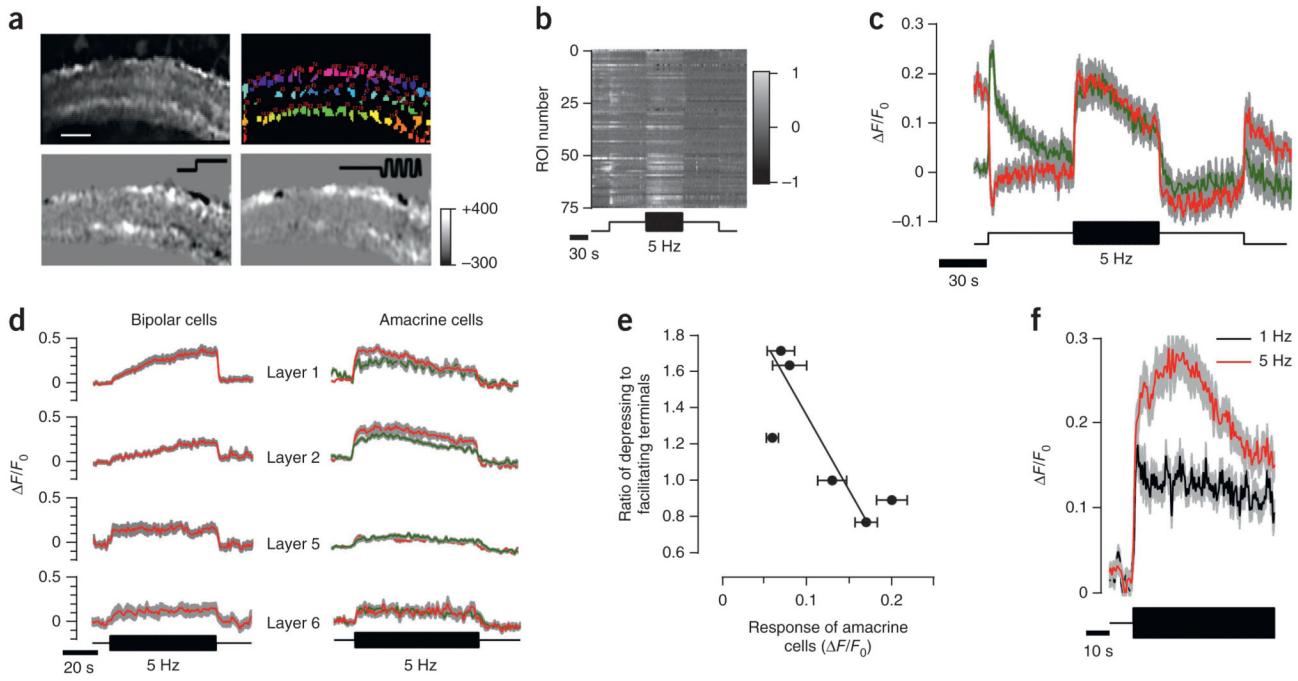

Figure 5. Stratification of amacrine cells synapses responding to contrast.

(**a**) Top, field of view showing SyGCaMP3 in synapses of amacrine cells and ROIs over puncate marked with different colors. Scale bar represents 15 μm. Bottom, difference images highlighting the change in SyGCaMP3 fluorescence in response to a step of light (left) and contrast (right). Color scale on the right indicates changes in fluorescence (arbitrary units). (**b**) Raster plot showing the relative change in fluorescence for each ROI shown in the bottom left image in **a**. (**c**) Average responses of ON (green) and OFF (red) amacrine cell synapses to a step of light and contrast (n = 158 and 175 terminals from 5 fish). (**d**) Right, average SyGCaMP3 response in ON (green) and OFF (red) amacrine cells in layers 1, 2, 5 and 6. Left, calcium dynamics in the same layers (from Fig. 4d). (**e**) Ratio of depressing to facilitating bipolar cell terminals (measured with sypHy) as a function of the amplitude of the initial response to contrast in amacrine cells. Each point represents averaged responses in one layer of the IPL calculated from 1,447 terminals from five fish. Data are fitted with a line (slope = −5.5 ± 1.95). (**f**) Amacrine cells adapted less and had smaller initial responses at lower temporal frequency (1 Hz, black, n = 64 terminals from 2 fish) than at high frequency (5 Hz, red, n = 230 terminals from 5 fish). Data represent responses from layer 2. Areas shaded gray indicate s.e.m.

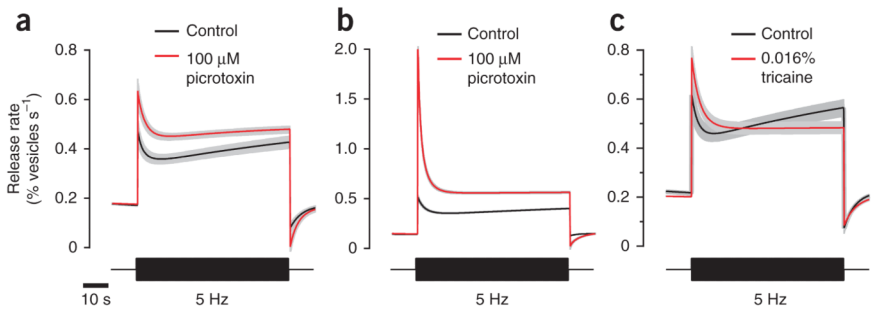

Figure 6. Pharmacological manipulation of the inhibitory input to bipolar cells removes facilitation.

(**a,b**) Release rate dynamics of OFF terminals from layers 1 and 2 in control conditions and in the presence of picrotoxin. Picrotoxin was dissolved in oxygenated Ames' solution and injected in the eye (**a**, *n* = 94 and 86 terminals, 3 fish) or added to bath solution (**b**, *n* = 380 and 135 terminals, 3 fish). (**c**) Release rate dynamics of terminals from layers 1 and 2 in control conditions and after application of 0.016% tricaine to the bath solution (*n* = 88 and 64 terminals, 5 fish). Note that the scale of the *y* axis in **b** is larger than that in **a** and **c**, and facilitation is therefore not as evident. Gray shaded areas indicate s.e.m.

Europe PMC Funders Author Manuscripts

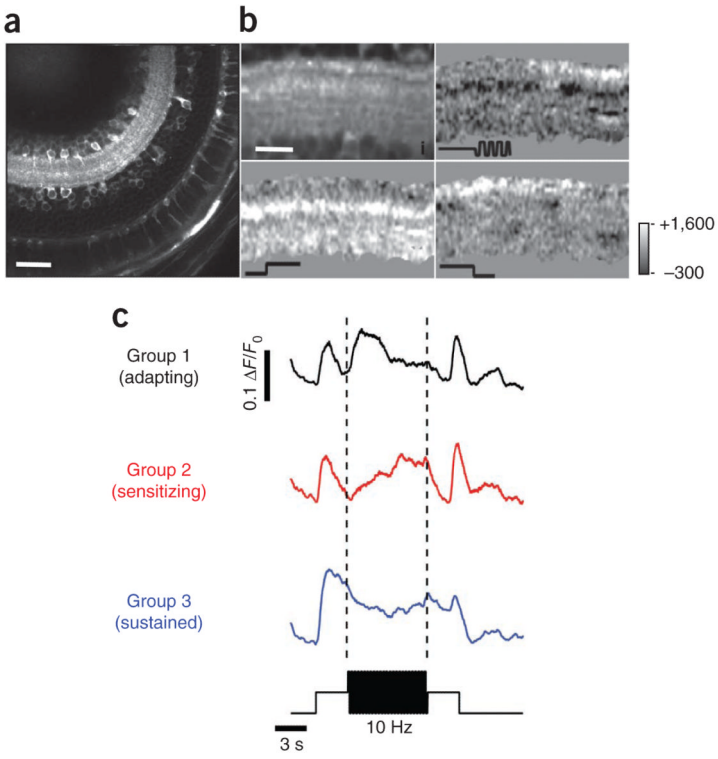

Figure 7. Depressing and facilitating responses in neurons postsynaptic to bipolar cells.

(**a**) Example of fish retina expressing GCaMP3 under the control of the *eno2* promoter. Scale bar represents 50 μm. (**b**) Field of view in a typical experiment (top left) and responses to light increment (top right), contrast increment (bottom left) and light decrement (bottom right). Each punctum in the top left image probably represents a compartment with high concentration of calcium channels. Scale bar represents 15 μm. (**c**) Dynamics of each voxel from **b** were clustered into three classes (7,552 voxels from 1 field of view). Responses were not initially separated into ON and OFF, as the majority of ganglion cells in zebrafish larvae are ON-OFF[32]. Note that timescale of this experiment is shorter than that shown in Figure 1c,d.

Europe PMC Funders Author Manuscripts

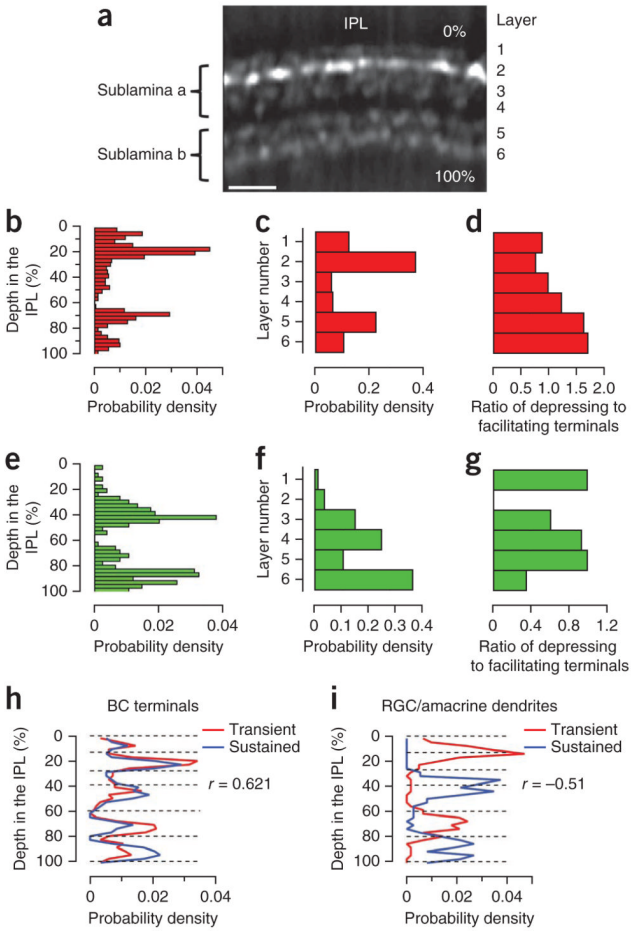

Figure 8. Stratification of different groups of bipolar cell terminals in the inner retina.

(**a**) A view of the IPL with bipolar cell terminals expressing sypHy (from Fig. 1a). The depth of the terminal in the IPL was measured from the photoreceptor side, and six layers could be recognized[43]. (**b,e**) The distribution of OFF (**b**) and ON (**e**) terminals as a function of depth (n = 824 and 255 terminals, 7 fish). (**c,f**) The distribution of OFF (**c**) and ON (**f**) terminals as a function of layer. The highest densities were in layers 1, 2, 5 and 6 for OFF terminals and 3, 4 and 5 for ON terminals. (**d,g**) Ratio of depressing to facilitating OFF (**d**) and ON (**g**) terminals calculated per layer from the response to a 5-Hz stimulus measured with sypHy. (**h**) Spatial distribution of bipolar cell terminals responding to contrast (red, transient, groups 1 and 2, n = 514 terminals, 7 fish) and those insensitive to contrast (blue, sustained, group 3, n = 198 terminal, 7 fish), as assessed in *ribeye-sypHy* fish. Note the high degree of overlap (correlation coefficient = 0.62). (i) Spatial distribution of transient and sustained (n = 191 and 131 terminals, 4 fish) responses in dendrites of ganglion cells and amacrine cells, as assessed in *eno2-SyGCaMP3* fish. Note the clear segregation (correlation coefficient = −0.51). Dashed lines indicate borders between layers.